

found to be concordant with susceptibility to CTL-3B6. Next, amino (N)- and (carboxyl) C-terminus-truncated minigenes encoding polypeptides around the polymorphic amino acid defined by the SNP were amplified by PCR from *SLC1A5* exon 1 cDNA as template and cloned into the above plasmid. The constructs all encoded a Kozak sequence and initiator methionine (CCACC-ATG) and for C-terminus deletions a stop codon (TAG).

For *UGT2B17*, a series of C-terminus deletion mutants with approximately 200 bp spacing was first constructed as above. For further mapping, N-terminus deletion mutants were added to the region that was deduced to be potentially encoding the CTL-1B2 epitope. For prediction of a CTL epitope, the HLA Peptide Binding Predictions algorithm on the Bioinformatics & Molecular Analysis Section (BIMAS) website (http://www-bimas.cit.nih.gov/molbio/hla_bind/)¹⁹ was utilized since HLA-A*0206 has a similar binding motif to that of A*0201.

Epitope reconstitution assay

The candidate mHag epitopes and allelic counterpart peptides (in case of *SLC1A5*) were synthesized by standard Fmoc chemistry. ⁵¹Cr-labeled mHag⁻ donor LCL were incubated with graded concentrations of the peptides and then used as targets in standard CRAs.

Results and Discussion

Statistical Approach and Estimation of Potential Overfitting

We reasoned that the mHag locus recognized by a given CTL clone could be defined by grouping LCLs from a HapMap panel into mHag⁺ and mHag⁻ subpanels according to their susceptibility to lysis by the CTL clone and then performing an association scan using the highly qualified HapMap data set containing over 3,000,000 SNP markers. The relevant genetic trait here is expected to show near complete penetrance, and the major concern with this approach arises from the risk of overfitting observed phenotypes to one or more incidental SNPs with this large number of HapMap SNPs under the relatively limited size of freedom due to small numbers of independent HapMap samples (90 for JPT+CHB and 60 for CEU and YRI, when not including their offspring).¹³

To address this problem, we first estimated the maximum sizes of the test statistics (here, χ^2 values) under the null hypothesis (i.e., no associated SNPs within the HapMap set) by simulating 10,000 case-control HapMap panels under different experimental conditions, and compared them with the expected size of test statistic values from the marker SNPs associated with the target SNP, assuming different linkage disequilibrium (LD), or r^2 values in between. As shown in Figure 1, the possibility of overfitting became progressively reduced as the number of LCLs increased, which would allow for identification of the target locus in a broad range of r^2 values, except for those mHags having very low minor allele frequencies (MAF) below ~ 0.05 . According to our estimation using the Phase II HapMap data (see Materials and Methods), the majority (>90%) of common target SNPs (MAF $> \sim 0.05$) could be captured by one or more HapMap SNPs with more than 0.8 of r^2 (Figure S1), ensuring a high probability of detecting an association (Figure 1, left panels). The simulation of pseudo-Phase II sets generated from the ENCODE regions provided a similar estimation¹³. False

positive and negative immunophenotyping results could also complicate the detection, reducing the expected test statistics through the “apparent” r^2 values (\hat{r}^2), as defined by

$$\hat{r}^2 = r^2 \times \frac{(1 - f_p - f_N)^2}{(1 - f_p + f_N q)(1 - f_N + f_p / q)} \quad (1)$$

, where f_p , f_N , and q represent false typing probabilities with positive and negative LCL panels, and the ratio of the positive to the negative LCL number, respectively. However, the high precision of cytotoxicity assays ($f_p \ll 0.1$, $f_N \equiv 0$) limits this drawback from the second term to within acceptable levels and allows for sensitive mHag locus mapping with practical sample sizes (Figure 1, middle and right panels), suggesting the robustness of our novel approach.

Evaluation of the Detection Power for Known mHags

Based on the above considerations, we then assessed whether this approach could be used to correctly pinpoint known mHag loci (Table S1). Since the relevant mHag alleles are common SNPs and directly genotyped in the Phase II HapMap set, or if not, located within a well-defined LD block recognized in this set (Figure S2), their loci would be expected to be uniquely determined with an acceptable number of samples, as predicted from Figure 1. To test this experimentally, we first mapped the locus for HA-1^H mHag⁷ by evaluating recognition of the HLA-A*0206-transduced HapMap cell panel with HLA-A*0206-restricted CTL-4B1.²⁰ After screening 58 well-growing LCLs from the JPT+CHB panel with CRAs using CTL-4B1 (Figure S3A, Table S2 and Table S3), we obtained 37 mHag⁺ and 21 mHag⁻ LCLs, which were tested for association at 3,933,720 SNP loci. The SNP (rs1801284) encoding the mHag is located within a HapMap LD block on chromosome 19q13.3, but is not

directly genotyped within this data set. The genome-wide scan clearly indicated a unique association with the HA-1^H locus within the *HMHA1* gene, showing a peak χ^2 statistic of 52.8 (not reached in 100,000 permutations) at rs10421359 (Figure 2A, 3A and Table S2, Table S3).

Identification of Novel mHags

We next applied this method to mapping novel mHags recognized by CTL clone 3B6, which is HLA-B*4002-restricted; and CTL clone 1B2, which is HLA-A*0206-restricted. Both clones had been isolated from peripheral blood samples of post-HSCT different patients. In preliminary CRAs with the JPT+CHB panel, allele frequencies of target mHags for CTL-3B6 and CTL-1B2 in this panel were estimated as ~25% and ~45%, respectively (data not shown). After screening 72 JPT+CHB LCLs with CTL-3B6, 36 mHag⁺ and 14 mHag⁻ LCLs were obtained, leaving 22 LCLs undetermined based on empirically determined thresholds (>51% for mHag⁺ LCLs and <11% for mHag⁻ LCLs) (Figure S3B and Table S2, S4). As shown in Figure 2B, the χ^2 statistics calculated from the immunophenotyping data produced discrete peaks in the LCL sets. The peak in chromosome 19q13.3 for the CTL-3B6 set showed the theoretically maximum χ^2 value of 50 (not reached in 100,000 permutations) at rs3027952, which was mapped within a small LD block of ~182kb, or more narrowly within its 35kb sub-block containing a single gene, *SLCIA5*, as a candidate mHag gene (Figure 3B). In fact, when expressed in 293T with HLA-B*4002 transgene, recipient-derived, but not donor-derived, *SLCIA5* cDNA was able to stimulate interferon- γ secretion from CTL-3B6 (Figure 4A), indicating that *SLCIA5* actually encodes the target mHag recognized by CTL-3B6. Conventional epitope mapping using a series of deletion mutants of *SLCIA5* cDNA finally identified an undecameric peptide, AEATANGGLAL, as the minimal epitope (Figure 4A). The donor-type AEPTANGGLAL induced IFN- γ with a 2-log lower efficiency, suggesting that AEPTANGGLAL may not be transported efficiently into the ER since endogenous

expression of a minigene encoding AEPTANGGLAL was not recognized by CTL-3B1 (Figure 4B). Unfortunately, although the peak statistic value showed the theoretically maximum value for this data set, it did not conform to the relevant SNP for this mHag (rs3027956) due to high genotyping errors of the HapMap data at this particular SNP. However, the result of our resequencing showed complete concordance with the presence of the rs3027956 SNP and recognition in the cytotoxicity assay (Table S4).

Similarly, 13 mHag⁺ and 32 mHag⁻ LCLs were identified from the screening of 45 JPT LCLs from the same panel using CTL-1B2 (Figure S3C and Table S2, S5). The χ^2 statistics calculated from the immunophenotyping data produced bimodal discrete peaks with this LCL set. The target locus for the mHag recognized by CTL-1B2 was identified at a peak (max $\chi^2 = 44$, not reached in 100,000 permutations) within a 598 kb block on chromosome 4q13.1, coinciding with the locus for a previously reported mHag, *UGT2B17*¹⁸ (Figure 2C and Figure 3C). In fact, our epitope mapping using *UGT2B17* cDNA deletion mutants (Figure 4C), prediction of candidate epitopes by HLA-binding algorithms¹⁹ (Figure 4D) and epitope reconstitution assays (Figure 4E), successfully identified a novel nonameric peptide, CVATMIFMI. Of particular note, this mHag was not defined by a SNP but by a CNV, i.e., a null allele,¹⁸ which is in complete LD with the SNPs showing the maximum χ^2 value (Table S5). Transplanted T cells from donors lacking both *UGT2B17* alleles are sensitized in recipients possessing at least one copy of this gene.¹⁸ Although LD between SNPs and CNVs has been reported to be less prominent,²¹ this is an example where a CNV trait could be captured by a SNP-based genome-wide association study.

The recent generation of the HapMap has had a profound impact on human genetics.^{13,15} In the field of medical genetics, the HapMap is a central resource for the development of theories and methods that have made well-powered genome-wide association studies of common human diseases a reality.²²⁻²⁸ The HapMap samples not only provide an

invaluable reference for genetic variations within human populations, but highly qualified genotypes that enable gene-wide scanning. Here, we have demonstrated how effectively HapMap resources can be utilized for genetic mapping of clinically relevant human traits. No imputations and tagging strategies are required^{25,28} and the potential loss of statistical power due to very limited sample sizes is circumvented by accurate immunological detection of the traits.

Using publicly available HapMap resources, high-throughput identification of mHag genes is possible without highly specialized equipment or expensive microarrays. Except for clinically irrelevant mHags with very low allele frequencies (e.g. MAF<5%), the target of a given CTL can be sensitively mapped within a mean LD block size, typically containing just a few candidate genes. The methodology described here will facilitate construction of a large panel of human mHags including those presented by MHC class II molecules, and promote our understanding of human allo-immunity and development of targeted allo-immune therapies for hematological malignancies.^{1,2} The HapMap scan approach may be useful for exploring other genetic traits or molecular targets (e.g., differential responses to some stress or drugs), if they can be discriminated accurately through appropriate biological assays. In this context, the recent report that we may reprogram the fate of terminally differentiated human cells²⁹ is encouraging, indicating possible exploration of genotypes that are relevant to cell types other than immortalized B cells.

Acknowledgements

We thank Drs. P. Martin and W. Ho for critically reading the manuscript; Ms. Keiko Nishida, Dr. Ayako Demachi-Okamura, Dr. Yukiko Watanabe, Ms. Hiromi Tamaki, and the staff members of the transplant centers for their generous cooperation and technical expertise. This study was supported in part by a Grant for Scientific Research on Priority Areas (B01)(no.17016089), from the Ministry of Education, Culture, Science, Sports, and Technology, Japan; Grants for Research on the Human Genome, Tissue Engineering Food Biotechnology and the Second and Third Team Comprehensive 10-year Strategy for Cancer Control (no. 26), from the Ministry of Health, Labour, and Welfare, Japan; a Grant-in-Aid from Core Research for Evolutional Science and Technology (CREST) of Japan.

Authorship

M.K. performed most of immunological experiments and analyzed data and wrote the manuscript; Y.N. performed the majority of genetic analyses and analyzed the data; H.T., T.K., M.Y., S.M. and K.T. performed research; K.T. contributed to the computational simulation; Y.I., T.T., K.M., Y.K. and Y.M. collected clinical data and specimens; T.I., H.T., S.R.R., T.T. and K.K. contributed to data analysis and interpretation, and writing of the article; Y.A. and S.O. supervised the entire project, designed and coordinated most of the experiments in this study, and contributed to manuscript preparation.

Conflict-of-interest disclosure: The authors declare no competing financial interests.

References

1. Bleakley M, Riddell SR. Molecules and mechanisms of the graft-versus-leukaemia effect. *Nat Rev Cancer*. 2004;4:371-380.
2. Spierings E, Goulmy E. Expanding the immunotherapeutic potential of minor histocompatibility antigens. *J Clin Invest*. 2005;115:3397-3400.
3. de Rijke B, van Horssen-Zoetbrood A, Beekman JM, et al. A frameshift polymorphism in P2X5 elicits an allogeneic cytotoxic T lymphocyte response associated with remission of chronic myeloid leukemia. *J Clin Invest*. 2005;115:3506-3516.
4. Marijt WA, Heemskerk MH, Kloosterboer FM, et al. Hematopoiesis-restricted minor histocompatibility antigens HA-1- or HA-2-specific T cells can induce complete remissions of relapsed leukemia. *Proc Natl Acad Sci U S A*. 2003;100:2742-2747.
5. Spierings E, Hendriks M, Absi L, et al. Phenotype frequencies of autosomal minor histocompatibility antigens display significant differences among populations. *PLoS Genet*. 2007;3:e103.
6. Brickner AG, Warren EH, Caldwell JA, et al. The immunogenicity of a new human minor histocompatibility antigen results from differential antigen processing. *J Exp Med*. 2001;193:195-206.
7. den Haan JM, Meadows LM, Wang W, et al. The minor histocompatibility antigen HA-1: a diallelic gene with a single amino acid polymorphism. *Science*. 1998;279:1054-1057.
8. Dolstra H, Fredrix H, Maas F, et al. A human minor histocompatibility antigen specific for B cell acute lymphoblastic leukemia. *J Exp Med*. 1999;189:301-308.
9. Kawase T, Akatsuka Y, Torikai H, et al. Alternative splicing due to an intronic SNP in HMSD generates a novel minor histocompatibility antigen. *Blood*. 2007;110:1055-1063.

10. Akatsuka Y, Nishida T, Kondo E, et al. Identification of a polymorphic gene, BCL2A1, encoding two novel hematopoietic lineage-specific minor histocompatibility antigens. *J Exp Med.* 2003;197:1489-1500.
11. Kawase T, Nanya Y, Torikai H, et al. Identification of human minor histocompatibility antigens based on genetic association with highly parallel genotyping of pooled DNA. *Blood.* 2008;111:3286-3294.
12. Risch N, Merikangas K. The future of genetic studies of complex human diseases. *Science.* 1996;273:1516-1517.
13. The International HapMap Project. *Nature.* 2003;426:789-796.
14. The International HapMap Project. A second generation human haplotype map of over 3.1 million SNPs. *Nature.* 2007;449:851-861.
15. The International HapMap Project. A haplotype map of the human genome. *Nature.* 2005;437:1299-1320.
16. Akatsuka Y, Goldberg TA, Kondo E, et al. Efficient cloning and expression of HLA class I cDNA in human B-lymphoblastoid cell lines. *Tissue Antigens.* 2002;59:502-511.
17. Riddell SR, Greenberg PD. The use of anti-CD3 and anti-CD28 monoclonal antibodies to clone and expand human antigen-specific T cells. *J Immunol Methods.* 1990;128:189-201.
18. Murata M, Warren EH, Riddell SR. A human minor histocompatibility antigen resulting from differential expression due to a gene deletion. *J Exp Med.* 2003;197:1279-1289.
19. Parker KC, Bednarek MA, Coligan JE. Scheme for ranking potential HLA-A2 binding peptides based on independent binding of individual peptide side-chains. *J Immunol.* 1994;152:163-175.

20. Torikai H, Akatsuka Y, Miyauchi H, et al. The HLA-A*0201-restricted minor histocompatibility antigen HA-1H peptide can also be presented by another HLA-A2 subtype, A*0206. *Bone Marrow Transplant.* 2007;40:165-174.
21. Redon R, Ishikawa S, Fitch KR, et al. Global variation in copy number in the human genome. *Nature.* 2006;444:444-454.
22. Barrett JC, Cardon LR. Evaluating coverage of genome-wide association studies. *Nat Genet.* 2006;38:659-662.
23. Nannya Y, Taura K, Kurokawa M, Chiba S, Ogawa S. Evaluation of genome-wide power of genetic association studies based on empirical data from the HapMap project. *Hum Mol Genet.* 2007;16:2494-2505.
24. Pe'er I, de Bakker PI, Maller J, Yelensky R, Altshuler D, Daly MJ. Evaluating and improving power in whole-genome association studies using fixed marker sets. *Nat Genet.* 2006;38:663-667.
25. Marchini J, Howie B, Myers S, McVean G, Donnelly P. A new multipoint method for genome-wide association studies by imputation of genotypes. *Nat Genet.* 2007;39:906-913.
26. Altshuler D, Daly M. Guilt beyond a reasonable doubt. *Nat Genet.* 2007;39:813-815.
27. Bowcock AM. Genomics: guilt by association. *Nature.* 2007;447:645-646.
28. de Bakker PI, Burt NP, Graham RR, et al. Transferability of tag SNPs in genetic association studies in multiple populations. *Nat Genet.* 2006;38:1298-1303.
29. Takahashi K, Tanabe K, Ohnuki M, et al. Induction of pluripotent stem cells from adult human fibroblasts by defined factors. *Cell.* 2007;131:861-872.
30. Sudo T, Kamikawaji N, Kimura A, et al. Differences in MHC class I self peptide repertoires among HLA-A2 subtypes. *J Immunol.* 1995;155:4749-4756.

Figure legends

Figure 1.

Numbers of positive and negative LCLs required for successful mHag mapping

The target locus was assumed to be uniquely identified, if the expected χ^2 value for the target SNP ($\hat{f}(i,j)$, see online Methods) exceeded the upper one percentile point of the maximum χ^2 values in 10,000 simulated case-control panels ($(g(i,j)^{P=0.01})$). Combinations of the numbers of mHag⁺ (vertical coordinates) and mHag⁻ (horizontal coordinates) samples satisfying the above condition are shown in color gradients corresponding to different max r^2 values between the target SNP and one or more nearby Phase II HapMap SNPs (r_{\max}^2), ranging from 0.4 to 1.0. Calculations were made for three HapMap population panels, CHB+JPT (top), YRI (middle), and CEU (bottom) and for different false positive and negative rates, $f_p = f_n = 0$ (left), $f_p = 0.1, f_n = 0$ (middle) and $f_p = 0.1, f_n = 0.05$ (right), considering the very low false negative assays for CRAs.

Figure 2.

Genome-wide scanning to identify chromosome location of mHag

χ^2 values were plotted against positions on each chromosome for each of three mHags recognized by CTL-4B1 (A), CTL-3B6 (B), and CTL-1B2 (C). Chromosomes are displayed in alternating colors. Threshold χ^2 values corresponding to the genome-wide $P = 10^{-3}$ (dark blue) and 10^{-2} (light blue), as empirically determined from 100,000 random permutations, are indicated by broken lines, while the theoretically possible maximum values are shown with red broken lines. The highest χ^2 value in each experiment is indicated by an arrow.

Figure 3.

Regions of mHag loci identified by HapMap scanning

LD structures around the SNPs showing peak statistical values (in JPT + CHB) are presented for each mHag locus identified with (A) CTL-4B1, (B) CTL-3B6, and (C) CTL-1B2. Regional χ^2 plots are also provided on the top of each panel. LD plots in pairwise $|D'|$ s with recombination rates along the segment were drawn with HaploView software 4.0 (<http://www.broad.mit.edu/mpg/haploview/>). The size and location of each LD block containing a mHag locus are indicated within the panels. Significant SNPs (blue letters), as well as other representative SNPs, are shown in relation to known genes. The positions of the SNPs showing the highest statistic values (red letters) are indicated by red arrow heads.

Figure 4.

Epitope mapping

(A) Determination of the *SLCIA5* epitope by deletion mapping. Plasmids encoding recipient full-length *SLCIA5*, exon 1 of recipient and donor, exon 1 with various N- and C-terminus deletions around the amino acid encoded by SNP rs51983014, and minigenes encoding AEATANGGLAL and its allelic counterpart AEPTANGGLAL were constructed and transfected into HLA-B*4002 transduced 293 T cells. Interferon (IFN)- γ was assessed by ELISA (right column) after co-culture of CTL-3B1 with 293T transfectants. (B) Epitope reconstitution assay with synthetic undecameric peptides, AEATANGGLAL and AEPTANGGLAL. (C) Structure of the *UGT2B17* gene and screening of *UGT2B17* cDNA and deletion mutants. HLA-A*0206-transduced 293T cells were transfected with each plasmid and co-cultured with CTL-2B1. IFN- γ production from CTL-1B2 (right column) indicated that the epitope was likely encoded by nucleotides 1448 -1586, including 30 nucleotides from position 1566 that could potentially encode part of the epitope. (D) Epitope

prediction using the HLA Peptide Binding Predictions algorithm.¹⁹ Since HLA-A*0201 and -A*0206 have similar peptide binding motifs,³⁰ the algorithm for HLA-A*0201 was used to predict candidate epitopes recognized by CTL-1B2. Values in parentheses indicate the predicted half-time of dissociation. (E) Epitope reconstitution assays with graded concentrations of synthetic nonameric peptides shown in panel D.

Figure 1

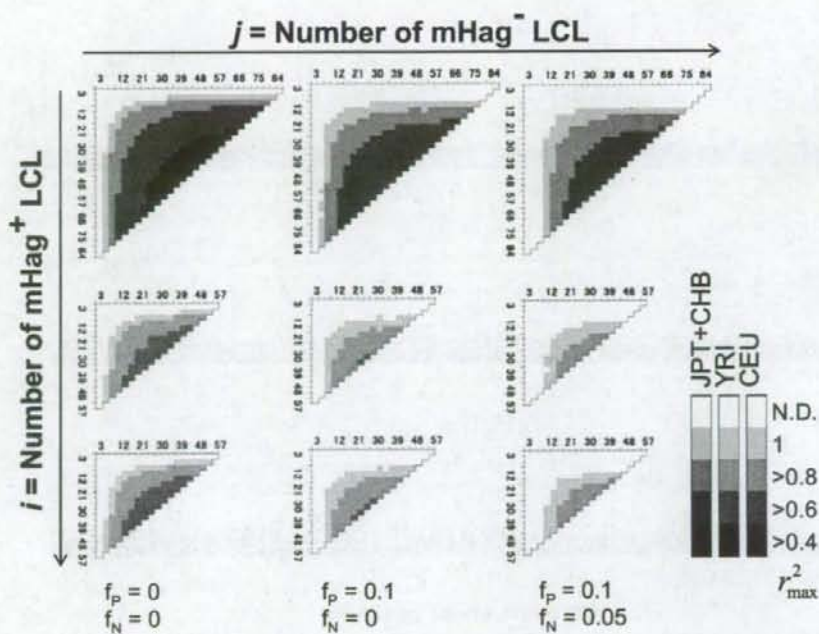


Figure 2

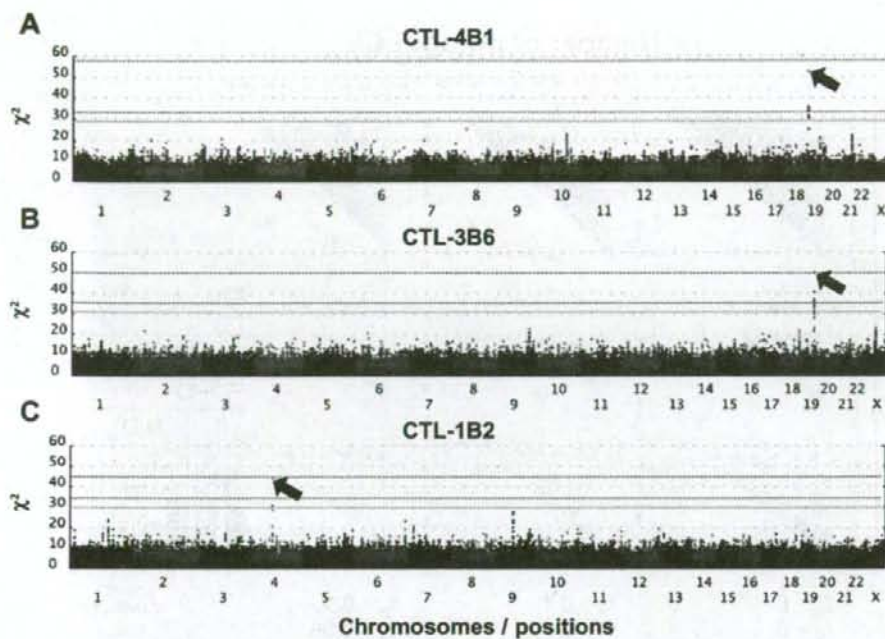


Figure 3

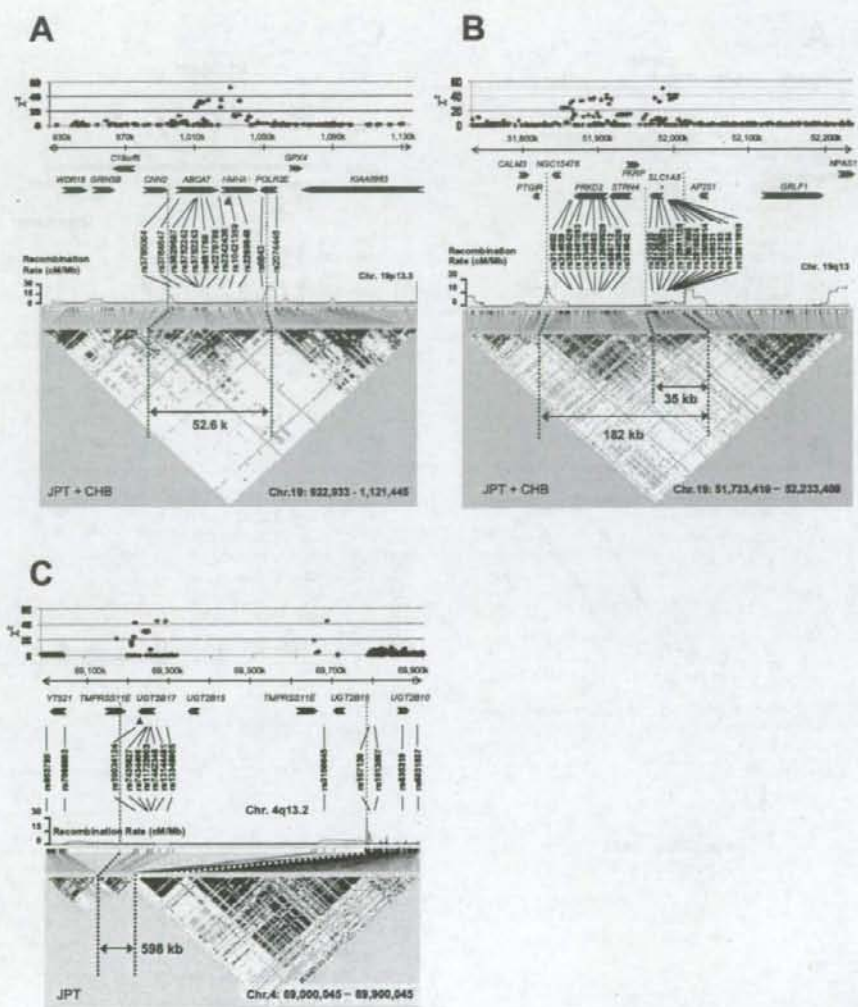
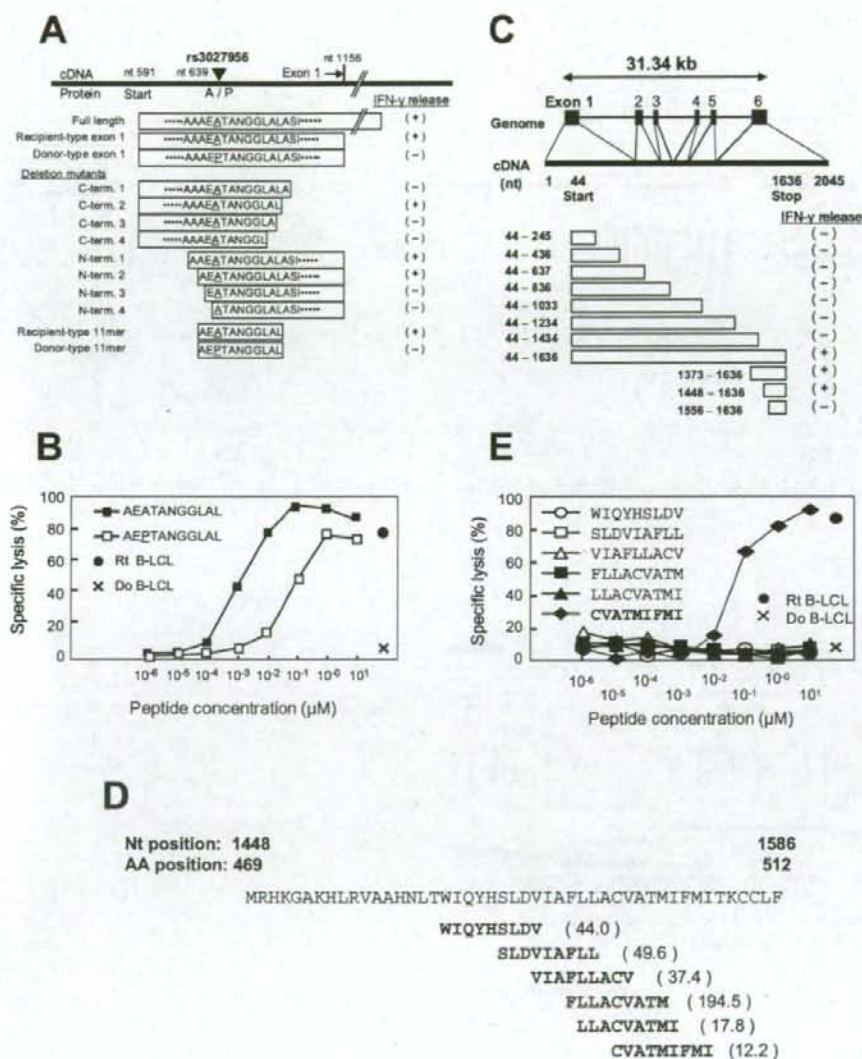


Figure 4



Decreased risk of acute graft-versus-host disease following allogeneic hematopoietic stem cell transplantation in patients with the 5,10-methylenetetrahydrofolate reductase 677TT genotype

Kyoko Sugimoto · Makoto Murata · Makoto Onizuka · Yoshihiro Inamoto · Seitaro Terakura · Yachiyo Kuwatsuka · Taku Ōba · Koichi Miyamura · Yoshihisa Kodera · Tomoki Naoe

Received: 23 October 2007 / Revised: 10 February 2008 / Accepted: 25 February 2008 / Published online: 26 March 2008
© The Japanese Society of Hematology 2008

Abstract Polymorphism in 5,10-methylenetetrahydrofolate reductase (MTHFR), a central enzyme in folate metabolism, has been shown to affect the sensitivity of patients to folate-based drugs such as methotrexate. In this study, we investigated whether a common single nucleotide polymorphism at position 677 in the donor or recipient's *MTHFR* gene affects the risk for acute graft-versus-host disease (GVHD) following allogeneic hematopoietic stem cell transplantation (HSCT) from HLA-identical sibling donors when the recipient receives prophylactic treatment with methotrexate for GVHD. *MTHFR* genotypes were determined in 159 recipients with a hematological disease and their donors using polymerase chain reaction–restriction fragment length polymorphism analysis of genomic DNA. The 677TT genotype, which encodes an enzyme with approximately 30% of the activity of the wild-type (677CC), was observed in 13% of patients and in 8% of normal donors. Multivariate analyses demonstrated a significant association between 677TT genotype in patients and a lower incidence of grade I–IV acute GVHD (relative risk, 0.35; 95% confidence interval, 0.13–0.95; $P = 0.040$).

There was no association between the incidence of acute GVHD and the donor *MTHFR* genotypes. These results suggest that greater immunosuppression by methotrexate due to low MTHFR enzyme activity decreases the risk of acute GVHD in recipients of allogeneic HSCT.

Keywords Methotrexate · Polymorphism · Frequency · Toxicity · Bone marrow transplantation · Peripheral blood stem cell transplantation

1 Introduction

Allogeneic hematopoietic stem cell transplantation (HSCT) is widely used to treat various hematological diseases, but patients can suffer from transplant-related complications including graft-versus-host disease (GVHD), treatment-related toxicities, and infection [1, 2]. The optimal matching of HLAs between the recipient and donor minimizes these complications, especially GVHD. Also, genetic polymorphism in non-HLA genes is now recognized as important [3]. Non-HLA genetic polymorphisms that can predict the risk and severity of GVHD are found in genes encoding minor histocompatibility antigens, pro- and anti-inflammatory cytokines, non-cytokine immunoregulators, and drug-metabolizing enzymes [4–7]. In a previous study, we analyzed the association between homozygous *glutathione S-transferase M1* and *T1* gene deletions in the recipient and donor with various outcomes of HSCT, and we found a significant association between the presence of the glutathione *S-transferase M1* enzyme in the recipients and higher treatment-related mortality (TRM) as well as a lower rate of survival [8]. In another study, we reported that a homozygous gene deletion leading to a null phenotype for the UDP-glycosyltransferase 2 family, polypeptide

K. Sugimoto · M. Murata (✉) · S. Terakura · T. Naoe
Department of Hematology and Oncology,
Nagoya University Graduate School of Medicine,
65 Tsurumai-cho, Showa-ku, Nagoya, Aichi 466-8550, Japan
e-mail: mmurata@med.nagoya-u.ac.jp

M. Onizuka · Y. Inamoto · Y. Kuwatsuka · T. Ōba ·
K. Miyamura · Y. Kodera
Department of Hematology, Japanese Red Cross
Nagoya First Hospital, Nagoya, Japan

M. Onizuka
Department of Hematology and Rheumatology,
Tokai University School of Medicine, Bouseidai, Japan

B17 enzyme [9], is an independent risk factor for higher TRM and lower survival after HSCT [10].

Here, we focused our attention on 5,10-methylenetetrahydrofolate reductase (MTHFR). MTHFR is a central regulatory enzyme in folate metabolism that converts 5,10-methylenetetrahydrofolate to 5,10-methyltetrahydrofolate [11]. A common functional polymorphism of the *MTHFR* gene occurs at C677T (alanine222valine) [12]. The 677TT genotype produces an enzyme with only 30% of the activity of the wild-type (677CC) enzyme in vitro and this decrease in activity leads to lower level of 5,10-methyltetrahydrofolate and an accumulation of 5,10-methylenetetrahydrofolate.

Methotrexate (MTX) is a folate pathway inhibitor and is as an important immunosuppressive agent used for prophylactic treatment of GVHD following HSCT [13]. MTX exerts its cytotoxic effect by inhibiting the activity of dihydrofolate reductase, which decreases intracellular levels of 5,10-methylenetetrahydrofolate (a substrate for thymidylate synthase), directly inhibits purine biosynthesis, and ultimately suppresses DNA synthesis [14]. The *MTHFR* C677T polymorphism has been shown to affect the sensitivity of patients to MTX. A recent study by Robien et al. of HSCT recipients from unrelated or related donors receiving prophylactic MTX for GVHD found that recipients with the *MTHFR* 677TT genotype have a lower incidence of acute GVHD [15]. Another study by Murphy et al. [16] of related HSCT recipients receiving MTX detected an association between the 677TT genotype in the donor but not the recipient, and a lower risk for GVHD. In contrast, a study by Pihusch et al. [17] of HSCT recipients from unrelated or related donors receiving MTX showed that the risk for acute GVHD was unrelated to the *MTHFR* C677T genotype in the recipient or donor. Thus, the influence of the *MTHFR* C677T polymorphism in the recipient and donor on GVHD remains controversial.

In this study, we analyzed the association between the *MTHFR* genotype either in recipients receiving MTX or their HLA-identical sibling donors with the outcome of HSCT. We found an association between the 677TT genotype in the recipient and a lower incidence of acute GVHD, but there was no association between the presence of this polymorphism in the donor and the outcome of HSCT.

2 Patients and methods

2.1 Patients

The study population included adult patients who had received bone marrow or peripheral blood stem cell transplantation from an HLA-identical sibling donor at the Nagoya University Hospital or the Japanese Red Cross Nagoya First Hospital between June 1987 and December

2006. A total of 159 patients and donor pairs were selected according to the following inclusion criteria: (1) short-term MTX and cyclosporin A were used as prophylaxis for GVHD; (2) an unmanipulated graft was transplanted; (3) DNA samples were stored and available for genotyping; and (4) clinical outcome data were available. All patients received scheduled doses of MTX as follows: 10 mg/m² on day 1, and 7 mg/m² on days 3 and 6 after transplantation, without leucovorin rescue. Dose reduction was not made in any patients. Cyclosporin A was administered intravenously at a dose of 3.0 mg/kg from day -1, and the doses were adjusted to maintain the whole blood trough level between 150 and 250 ng/ml until the patient tolerated oral administration. If the patient had neither uncontrollable GVHD nor gastrointestinal damage, cyclosporin A was given orally and then decreased gradually. Discontinuation of cyclosporin A due to its toxicity or for induction of graft-versus-leukemia effect was not done in any patients.

The characteristics of the patients are summarized in Table 1. One hundred and forty-three patients were treated for malignant diseases and 77 were classified as having

Table 1 Patient characteristics

	n = 159
Age, median, y (range)	38 (15-62)
Sex, n	
Male	90
Female	69
Disease, n	
Malignant	
Acute myeloid leukemia	48
Acute lymphoblastic leukemia	28
Chronic myeloid leukemia	39
Myelodysplastic syndrome	16
Multiple myeloma	5
Non-Hodgkin's lymphoma	5
Hodgkin's lymphoma	1
Adult T cell leukemia	1
Non-malignant	
Severe aplastic anemia	15
Paroxysmal nocturnal hemoglobinuria	1
Status of malignant disease, n	
Standard	77
Advanced	66
Pretransplant conditioning regimen, n	
Myeloablative regimen	139
Non-myeloablative regimen	20
Stem cell source, n	
Bone marrow	122
Peripheral blood	37

standard-risk diseases, including acute myeloid leukemia in first remission ($n = 24$), acute lymphoblastic leukemia in first remission ($n = 18$), chronic myeloid leukemia in first chronic phase ($n = 32$), and myelodysplastic syndrome classified as refractory anemia ($n = 3$). All other hematological malignancies were considered as advanced diseases. Twenty patients received a fludarabine-including regimen with 2 Gy of total body irradiation or without total body irradiation, which was defined as a non-myeloablative regimen.

Patients who achieved neutrophil recovery ($\geq 500/\mu\text{l}$) after transplantation were evaluated for acute GVHD, and patients who survived at least 100 days after transplantation were evaluated for chronic GVHD. Acute and chronic GVHD were graded according to standard criteria [18, 19]. TRM was defined as any death that occurred while the patient was in remission. Relapse-free survival (RFS) was defined as the number of days from transplantation to disease progression or death from any causes other than disease progression. Overall survival (OS) was defined as the number of days from transplantation to death from any cause. Common Terminology Criteria for Adverse Events version 3.0 was used to assess the severity of mucositis/stomatitis and abnormality of laboratory data including bilirubin, aspartic transaminase, alanine transaminase, and alkaline phosphatase based on the peak level within 14 days after transplantation [20]. Informed consent was obtained from all patients and donors, and the study was approved by the ethics committees at Nagoya University School of Medicine and Japanese Red Cross Nagoya First Hospital.

2.2 Determination of the MTHFR C677T polymorphism

The MTHFR C677T polymorphism was determined by polymerase chain reaction (PCR)-restriction fragment length polymorphism method using genomic DNA from donor and patient cells as described previously [12]. The sense and antisense primers used for PCR were 5'-TGAA GGAGAAGGTGTCTGCGGGA-3' and 5'-AGGACGGTG CCGTGAGAGTG-3', respectively. Each PCR (20 μl total volume) contained 0.4 μl of Advantage 2 Polymerase Mix (Clontech Laboratories, Inc., Mountain View, CA, USA), 0.2 mmol/l of each of the four deoxyribonucleotide, 10 pmol of each primer for MTHFR, 2 μl of 10 \times Advantage 2 PCR buffer, and 0.5 μl genomic DNA extracted from peripheral blood or bone marrow before transplantation or from Epstein-Barr virus-transformed lymphoblastoid cells established from pretransplant cryopreserved peripheral blood mononuclear cells. Amplification was carried out for 30 cycles of denaturation at 95°C for 30 s, annealing at 68°C for 10 s, and elongation at 72°C for 15 s on a model

9600 thermocycler (Perkin-Elmer, Norwalk, CT, USA). After amplification, the 198-bp MTHFR fragment was digested overnight at 37°C with 10 units of *Hinf*I (New England BioLabs, Inc., Ipswich, MA, USA) in a 20- μl reaction containing 17 μl of PCR fragment and 2 μl of 10 \times NEBuffer 2. A 15- μl sample of the digestion products was analyzed by electrophoresis on a 2% agarose gel. Wild-type (CC) individuals were identified by the presence of only a 198-bp fragment, heterozygotes (CT) by the presence of both 175/23 and 198-bp fragments, and homozygotes (TT) by the presence of only the 175 and 23-bp fragments.

2.3 Statistical analysis

A chi-square test with 2 \times 2 contingency tables was used to evaluate differences in the frequencies of MTHFR C677T polymorphism between patients and donors. The Cox proportional hazard model was applied to univariate and multivariate analyses to identify risk factors for acute GVHD (grade I-IV or II-IV), chronic GVHD, TRM, relapse, RFS, OS, mucositis/stomatitis (grade 1-4, 2-4, or 3-4), and abnormality of bilirubin, aspartic transaminase, alanine transaminase, and alkaline phosphatase (grade 1-4 or 2-4) [21]. All variables with $P < 0.10$ were entered into the multivariate logistic regression. The following variables were evaluated: patient age (continuous variable), year of transplantation (continuous variable), disease (non-malignant disease vs. malignant disease), disease status of hematological malignancy at the time of transplantation (advanced disease vs. standard disease), pretransplant conditioning regimen (non-myeloablative regimen vs. myeloablative regimen), stem cell source (bone marrow vs. peripheral blood), acute GVHD (grade I-IV vs. grade 0 and grade II-IV vs. grade 0-I), patient MTHFR genotype (TT vs. CC/CT and TT/CT vs. CC), and donor MTHFR genotype (TT vs. CC/CT and TT/CT vs. CC). $P < 0.05$ was regarded as including a statistically significant difference, and P value between 0.05 and 0.1 as suggesting a trend. The incidence of acute GVHD was analyzed using the Kaplan-Meier method, and log rank test was used to analyze the differences [22].

3 Results

3.1 Frequencies of MTHFR C677T genotypes

The frequencies of the CC, CT, and TT genotypes in the patients and donors are summarized in Table 2. There was no significant difference in the distribution pattern of the C677T genotypes between all patients and donors ($P = 0.19$). In the patients with myelodysplastic syndrome, the frequency of the CC genotype was 56%, which was